LETTER • OPEN ACCESS

Greenhouse gas footprints of utility-scale photovoltaic facilities at the global scale

To cite this article: Joyce H C Bosmans *et al* 2021 *Environ. Res. Lett.* **16** 094056

View the article online for updates and enhancements.

ENVIRONMENTAL RESEARCH
LETTERS

CrossMark

LETTER

Greenhouse gas footprints of utility-scale photovoltaic facilities at the global scale

Joyce H C Bosmans*, Louise C Dammeier and Mark A J Huijbregts

Department of Environmental Science, Faculty of Sciences, Radboud University Nijmegen, Heyendaalseweg 135, 6525 AJ Nijmegen, The Netherlands
* Author to whom any correspondence should be addressed.

E-mail: Joyce.Bosmans@ru.nl

Abstract

Technological characteristics and meteorological conditions are major determinants of the greenhouse gas (GHG) footprints of photovoltaic facilities. By accounting for technological and meteorological differences, we quantified the GHG footprints of 9992 utility-scale photovoltaic facilities worldwide. We obtained a median greenhouse gas footprint of 58.7 g CO_2-eq kWh^{-1}, with a 3-fold spread (28.2–94.6 g CO_2-eq kWh^{-1}, 2.5th and 97.5th percentiles). Differences in panel type appeared to be the most important determinant of variability in the GHG footprint, followed by irradiation and a facility's age. We also provided a meta-model based on these three predictors for users to determine the facility-specific greenhouse gas footprint. The total cumulative electricity produced by the utility-scale photovoltaic fleet worldwide is 457 TWh yr^{-1}, 99.6% of which is produced at footprints below 100 g CO_2-eq kWh^{-1}. Compared to earlier studies, the footprints we computed of global utility-scale facilities show a relatively large spread. In order to further improve the accuracy of facility-specific footprints, more information on panel type as well as production country is required.

1. Introduction

Photovoltaic solar power (PV) is an important source of renewable energy, producing electricity at much lower greenhouse gas (GHG) emissions than conventional fossil-based technologies [1]. By 2019, global PV capacity reached 580 GW [2] and generated ~720 TWh of electricity, roughly 3% of current global electricity production [3]. PV is now the third-largest renewable electricity source after hydropower and onshore wind [4], and its share is growing rapidly, with a potential 877 GW added by 2024, accounting for 60% of the expected growth of all renewables [3].

Various studies have investigated how life-cycle GHG emissions of PV compare to emissions from fossil-based electricity sources. One approach in such studies is to perform a meta-analysis by gathering case studies reported in literature and harmonize their findings to represent standardized system boundaries for irradiation, lifetime, performance ratio and/or module efficiency [5–8]. The GHG footprints in these

papers, expressed as life-cycle GHG emissions per unit of electricity produced, range from ~14 to 82 g CO_2-eq kWh^{-1} under harmonized conditions, with the greatest source of variation being the type of panel [7, 9, 10]. Typically, thin film panels such as cadmium telluride, copper indium gallium diselenide and amorphous silicon have lower GHG footprints than mono- and poly-crystalline silicon panels.

Meta-analyses provide insights in the sources of life-cycle GHG emissions related to PV, but because of the harmonization process they do not show how footprints can vary in reality. Location of installation determines the amount of irradiation received by the panels, and location of production determines the GHG emissions during manufacturing, both important factors in the PV GHG footprints [10–14]. Furthermore, intra-type variation in module efficiency, type of mounting system, lifetime, degradation and capacity can explain variations in PV GHG footprints [5, 15–20]. With higher irradiation, for instance, footprints reduce due to higher electricity production [5, 10–13, 17, 18]. Spatial differences

in environmental footprints of PV are assessed by Louwen *et al* [21] for rooftop PV in Eurasia and Africa, Ito *et al* [22] for two sites in France and Moroco, and Pérez-López *et al* [23], Perez-Lopez *et al* [24] for utility-scale PV globally. These studies indicate that GHG footprints of PV vary significantly with location. Placing a PV facility at a location with high irradiation can reduce the GHG footprint by up to ∼75% [21], and even within a country such as France choosing a location with higher irradiation can reduce the footprint by ∼25% [23]. While providing valuable insights into the geographic variation of PV footprints, these studies do not use data on the actual fleet of PV facilities, and therefore cannot assess the footprint of actual PV electricity.

Here, we quantified life-cycle GHG footprints of the global utility-scale PV fleet, including ∼10 000 facilities. With these GHG footprints we derived GHG emission—electricity supply curves for the PV fleet and built a regression model to analyse which technological and/or climatological variables are most important for determining the GHG footprint. In addition, this regression model can be used for quick estimation of GHG footprints of PV. We use 30 years of the most recent high-resolution climate reanalysis dataset ERA5 [25] at ∼0.25° spatial and hourly time resolution, as well as a global dataset on facility-specific location and technological characteristics of existing and planned utility-scale facilities, combined with regionalized life-cycle inventory data for PV production.

2. Materials and methods

2.1. GHG footprint
We compute the GHG environmental footprint EF_{GHG} as impact I per unit of electric power P:

$$EF_{GHG} = \frac{I}{P} \qquad (1)$$

where we consider life-cycle impact I in g CO_2-eq, and lifetime electricity output P of a PV facility in kWh. For a location-specific EF, we use a dataset of 9992 utility-scale photovoltaic parks across the globe (see section 2.2), market shares by origin countries per continent [26] and production location-specific impact I (this section), as well as a high-resolution global climate reanalysis dataset (see section 2.3). Figure 1 provides an overview of our methods.

Life-cycle greenhouse gas emissions, or impact I in equation (1), are derived using market shares by origin countries per continent [26] and production location-specific impact (see SI section B for further details) and a facility's panel surface area:

$$I = I_{m^2} \cdot A \qquad (2)$$

with surface area A (m²) depending on a facility's capacity and efficiency:

$$A = \frac{Wp}{rsds_{STC} \cdot \eta} \qquad (3)$$

following Bhandari *et al* [7]. Capacity in Wp is available from the Wiki-Solar dataset ('Wp' for Watt-peak, indicating direct current output under standard testing conditions), $rsds_{STC}$ is surface downward solar radiation under standard testing conditions (1000 W m^{-2}) and η is panel efficiency (as a fraction of solar radiation that the panel can convert into electricity). η depends on panel type and year, following Chen *et al* [27], see SI section A.

We derived for each panel type considered (mono-crystalline silicon, poly-crystalline silicon, amorphous silicon, cadmium telluride and copper indium (gallium) diselenide life cycle GHG emissions (I_{m^2}) representing a continent-specific weighted average of production countries, as data on the production location for each individual facility is unavailable. Market shares by producing countries per continent are obtained from Absolute Reports [26]. We use 2016 market shares for current facilities, and 2019 market shares for planned facilities. Type-specific impacts per producing country (China, EU, US, Malaysia and Korea) are obtained from literature (see SI table B1).
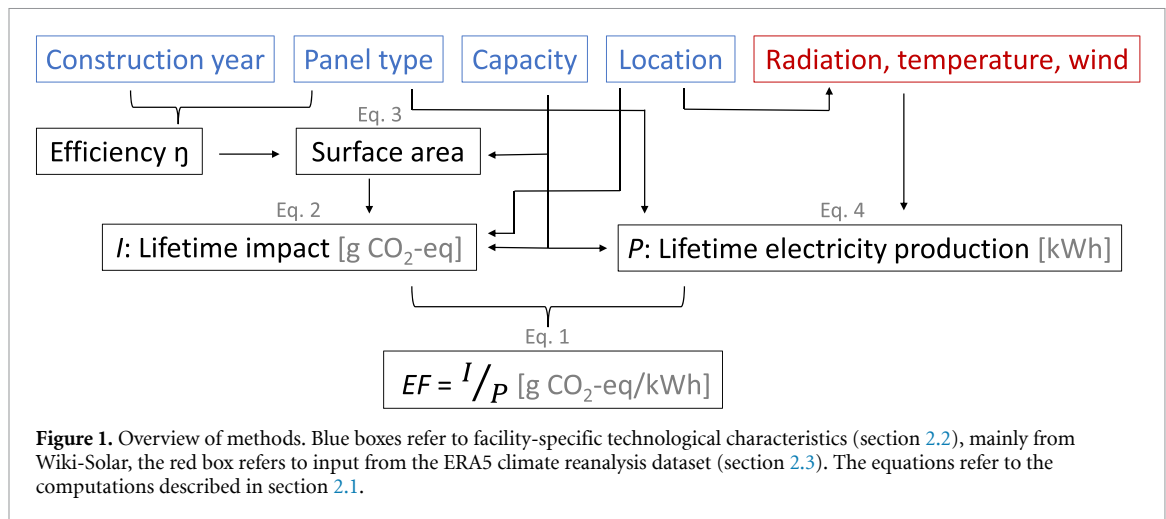
Besides the impacts per m² of panel, a PV facility's impact derives from the so-called 'balance of systems' (BOS). The BOS includes the mounting system, wiring and inverters [5]. Here we use EcoInvent 3.5 values per m² of open-ground mounting system as well as the impacts of inverters and electrical installation per unit capacity, independent of panel type and production location.

For more detail on life-cycle GHG emissions, see SI section B.

The electricity output of a PV facility depends on multiple variables, including the panel type, irradiation and temperature. Here we follow the PV power computations of Jerez *et al* [28], based on Mavromatakis *et al* [29]. Jerez *et al* [28] define the PV power generation potential PVpot, a dimensionless magnitude accounting for the performance of a PV cell with respect to the power capacity (here expressed in MWac, obtained from the WikiSolar database). PVpot depends on radiation rad and cell temperature T_{cell}, the latter depending on air temperature, radiation and wind [30] as well as panel type. We furthermore account for losses due to panel degradation. In short, the instantaneous PV power production provided to the grid (in alternating current) is given by:

$$P(t) = PVpot(rad, T_{cell}) \cdot MWac \cdot f_{loss}. \qquad (4)$$

For PVpot we use the location-specific hourly ERA5 climate variables for 1988–2017 (see section 2.3), thus obtaining a power output representative of current climate. Loss ratio f_{loss} is applied to account for panel degradation and is set to 0.899, representing a loss of

Figure 1. Overview of methods. Blue boxes refer to facility-specific technological characteristics (section 2.2), mainly from Wiki-Solar, the red box refers to input from the ERA5 climate reanalysis dataset (section 2.3). The equations refer to the computations described in section 2.1.

0.7% yr^{-1} over a 30 years lifetime [23, 31]. A 30 year lifetime is assumed to be representative of modern PV [31]. The full equations for computing generated electricity are given in SI section C.

2.2. Facility-specific technology and location data

To compute facility-specific impact I and power output P, we need to know a facility's age (construction year), panel type, capacity and location-specific climate variables (see figure 1). We use the Wiki-Solar dataset (http://wiki-solar.org) which provides technological characteristics of utility-scale PV projects around the globe, with a minimum, median and maximum capacity of 3, 10 and 3000 MWp. Wiki-Solar includes 10 268 PV facilities, of which 9992 with a known location. 7982 facilities are operating or were in late stages of construction at the time of data-gathering (2019) and 2010 are planned. The median construction year is 2016. The total capacity in these 9992 facilities is 367 GWp. Figure 2 shows the location and capacities of all facilities.

The Wiki-Solar dataset provides information on the panel type for 1249 out of 9992 facilities. We consider the five most common types [32]; mono-crystalline silicon, poly-crystalline silicon, amorphous silicon, cadmium telluride and copper indium (gallium) diselenide. To increase the number of facilities with known panel type, we gathered extra information from PV suppliers in Wiki-Solar as well as US EIA and GEO datasets [33, 34]. We found specific panel types for 99 additional facilities, and narrowed the panel type to either crystalline or thin film for 1443 and 17 facilities, respectively. Where a specific type is unknown, we computed the GHG footprint for the two crystalline types in case of crystalline panels, the three thin film types in case of thin film panels, or all five types where no information on panel type was found. The results represent an average footprint of these types weighted by 2016 production data for current facilities and 2019 production data for planned facilities (see SI table A2). As

described above in section 2.1, results also represent a continent-specific weighted average of I_{panel} by production countries.

For capacity, Wiki-Solar provides both MWac and MWp for 2046 facilities. For these facilities, the median performance ratio (PR = MWac/MWp) is 0.8, which is also the IEA recommended value [31]. For all remaining facilities, either MWac or MWp is given, and the PR value of 0.8 is used to derive the missing MWac or MWp.
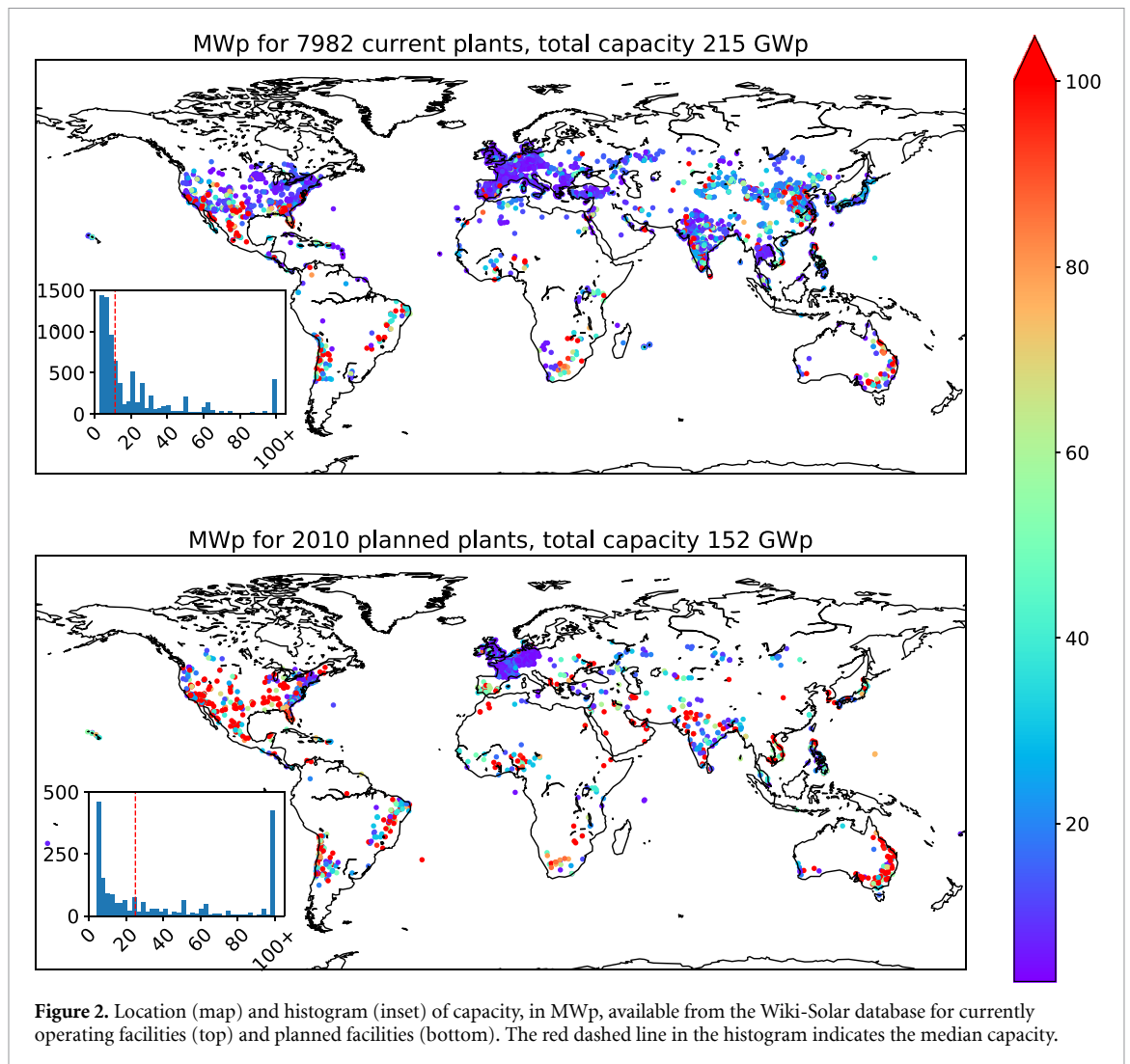
For more detail on the Wiki-Solar dataset and gap filling, see Supplementary Information section A (available online at stacks.iop.org/ERL/16/094056/mmedia).

2.3. Climate data

For power output computation, we use the most recent and highest-resolution global re-analysis dataset representing current climate at $0.25° \times 0.25°$ (roughly 30×30 km at equator) [25], obtained through the Copernicus Climate Change Service [35]. Hourly resolution allows us to include the daily cycle of radiation as well as temporal variation in cell efficiency due to cell temperature (including air temperature, radiation and wind, see SI section C [36]. Hourly data gives improved estimates of PV power generation compared to lower-resolution data [37] (for more detail see SI section D).

2.4. GHG emission—supply curves

To create GHG emission—supply curves, we ordered all 9992 by their GHG footprint and computed the cumulative power production. Furthermore, we applied a bootstrapping technique to determine the uncertainty introduced by panel type, which is unknown for a large number of facilities. Instead of using weighted footprints at facilities where panel is unknown, we created 10 000 instances of our dataset, where each time a facility's footprint (if unknown) is set to that of one of the panel types, selected using 2016 (2019) production data as weights for current (planned) facilities (Fraunhofer ISE [32], also used

Figure 2. Location (map) and histogram (inset) of capacity, in MWp, available from the Wiki-Solar database for currently operating facilities (top) and planned facilities (bottom). The red dashed line in the histogram indicates the median capacity.

in the weighted footprints in section 3.1). 2016 is the median construction year for facilities with unknown type in the Wiki-Solar database, 2019 is the latest year for which type-specific production data is available (see SI table A2).

2.5. Regression analyses
After computing the GHG footprint for utility-scale PV facilities, we created a linear regression model to help determine which of the predictors we take into account (age, panel type, capacity and location-specific climate variables, see figure 1) explains most of the variance in EF_{GHG}. We build this model on the 1348 facilities for which panel type is known. Note that we cannot currently take production location into account in this regression, as facility-specific production location is unknown (instead we used continent-specific weighted averages of production countries based on market shares). For the climate variables, we use location-specific 30-year mean daytime irradiation I, temperature T and wind speed u as well a coefficient of variation (CV) for each variable to represent intra-year variation (see SI equation 6). The correlation matrix of the predictors (supplementary
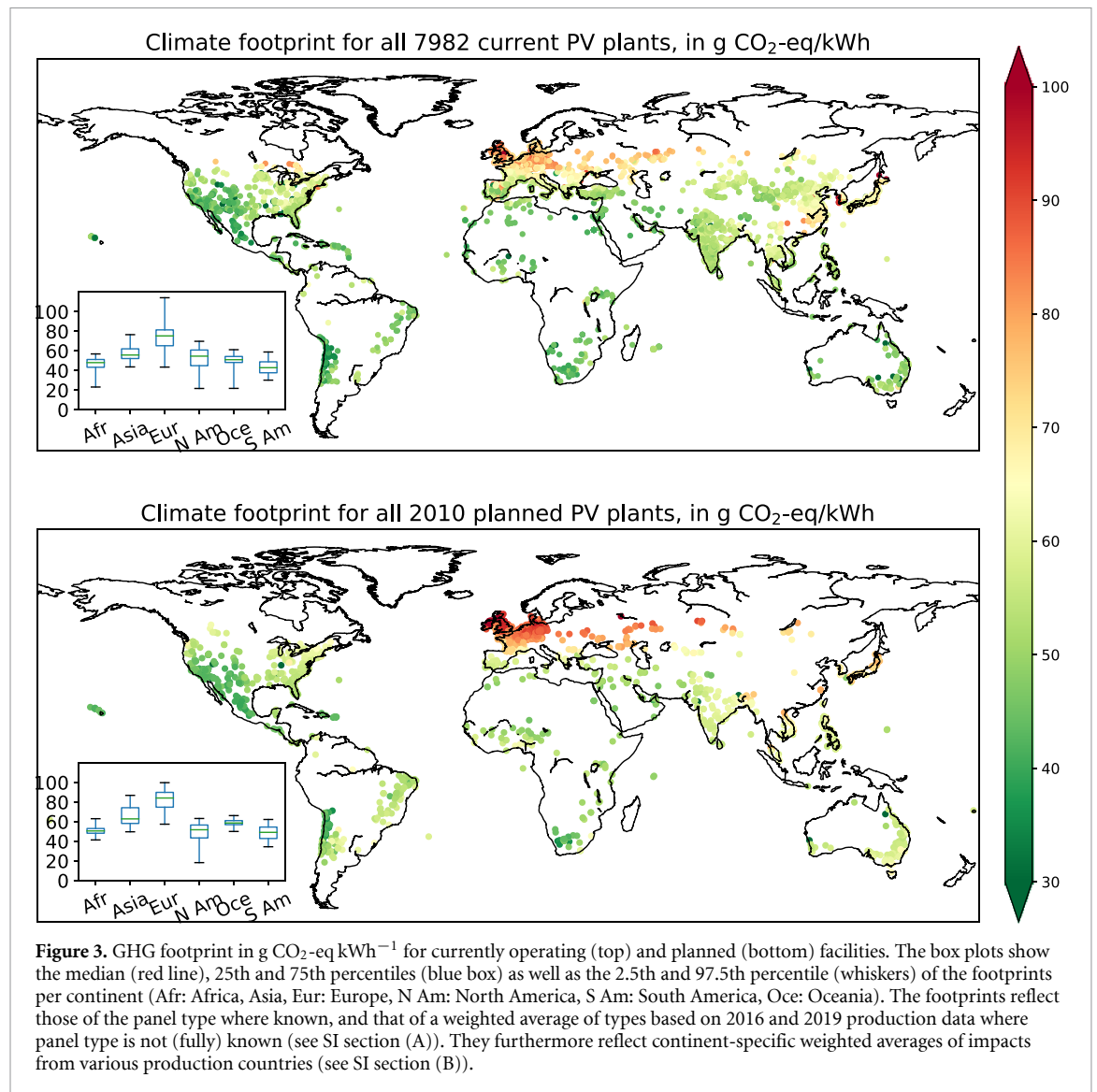
figure E1) shows that there are no significant correlations between the variables, and the variance inflation factors (vifs) are all below 5. Capacity is log-transformed because its distribution is right-skewed. We also log-transformed the response variable (EF_{GHG}). The model includes the interaction between panel type and construction year, because these together determine efficiency η used in the life-cycle GHG emissions (equation (3), SI section A).

After determining the best model, based on the Akaike Information Criterion, we assess the importance of each predictor using predictor randomization. Each predictor is randomized in turn, after which the model is re-built. The larger the drop in the model's R^2, the more important a predictor is. Results are shown in section 3.3 and more details on the regression model can be found in Supplementary section E.

3. Results

3.1. GHG footprints
The GHG footprint of all PV facilities is 58.7 (28.2–94.6) g CO_2-eq kWh^{-1} (median, 2.5%–97.5%

Figure 3. GHG footprint in g CO_2-eq kWh^{-1} for currently operating (top) and planned (bottom) facilities. The box plots show the median (red line), 25th and 75th percentiles (blue box) as well as the 2.5th and 97.5th percentile (whiskers) of the footprints per continent (Afr: Africa, Asia, Eur: Europe, N Am: North America, S Am: South America, Oce: Oceania). The footprints reflect those of the panel type where known, and that of a weighted average of types based on 2016 and 2019 production data where panel type is not (fully) known (see SI section (A)). They furthermore reflect continent-specific weighted averages of impacts from various production countries (see SI section (B)).
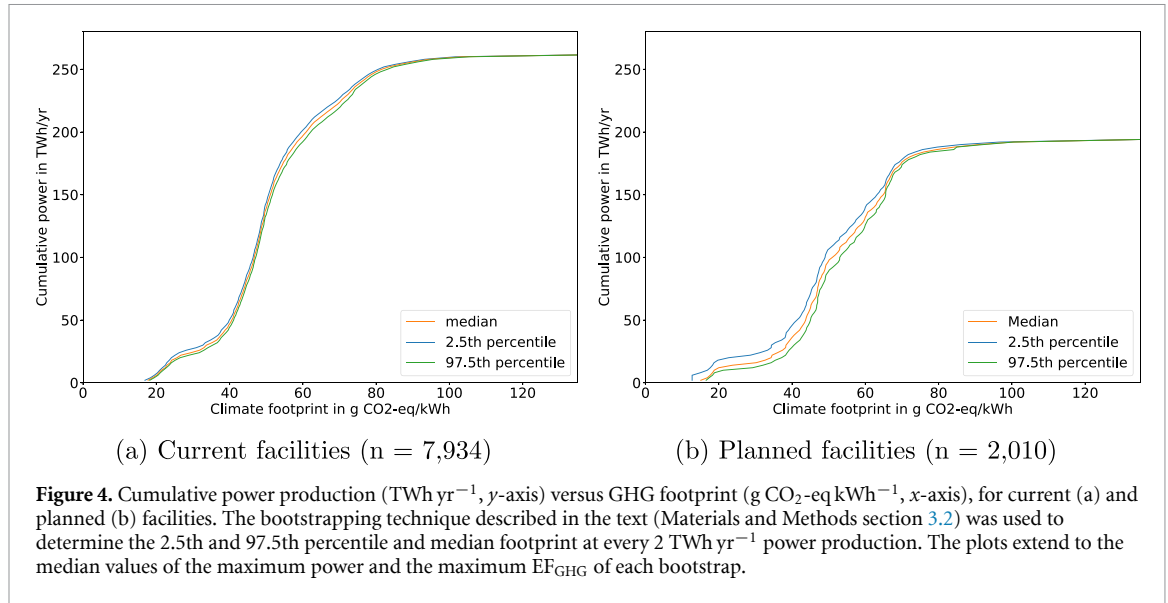
quantiles). 9810 out of the 9992 facilities (98.2%) have a GHG footprint below 100 g CO_2-eq kWh^{-1}. Figure 3 shows that the spatial pattern is mostly dominated by latitude, with facilities at higher latitudes having higher GHG footprints due to lower irradiation and electricity output. The latitudinal pattern also emerges by looking at GHG footprints per continent (box plots in figure 3); Europe has the highest footprint, with a median EF_{GHG} of 76.9 (46.1–112.2) g CO_2-eq kWh^{-1} (based on current and planned facilities combined). Lowest footprints are found in low-latitude continents; South America (45.4 [30.6–62.3] g CO_2-eq kWh^{-1}) and Africa (49.1 [31.5–61.0] g CO_2-eq kWh^{-1}).

Besides latitude, panel type also has a great influence on EF_{GHG}. As a sensitivity analysis, we assessed the non-weighted footprints of the 7148 facilities of unknown type, for which footprints were computed for all five types, across types and continents. This indicates that panel type can have a larger effect on GHG footprints than location of installation;

choosing cadmium telluride in Europe can result in lower footprints (35.9 [23.0–51.7] g CO_2-eq kWh^{-1}) than choosing mono-crystalline panels in South America (57.9 [44.0–74.7] g CO_2-eq kWh^{-1}), despite facilities in South America receiving much higher irradiation than those in Europe (2165 vs 1135 kWh m^{-2} yr^{-1}, median values).

Differentiating between operating and planned facilities indicates slightly lower footprints for current facilities (58.4 [27.1–93.3]) compared to planned facilities (60.1 [38.4–95.6]). This increase occurs despite an increase in panel efficiency, which causes lower footprints for newer facilities of all individual panel types. However, across all facilities, the increase in market share of mono-Si panels (see SI table A2), which have the highest impacts of all panel types, causes footprints to increase. Also, in Europe a higher share of planned facilities is produced in China, further increasing EF_{GHG}. In North America the opposite happens; footprints drop as imports shift from China to production locations with lower impacts.

Figure 4. Cumulative power production (TWh yr^{-1}, *y*-axis) versus GHG footprint (g CO$_2$-eq kWh^{-1}, *x*-axis), for current (a) and planned (b) facilities. The bootstrapping technique described in the text (Materials and Methods section 3.2) was used to determine the 2.5th and 97.5th percentile and median footprint at every 2 TWh yr^{-1} power production. The plots extend to the median values of the maximum power and the maximum EF$_{GHG}$ of each bootstrap.

3.2. GHG emission—supply curves

The GHG emission supply curves show that all facilities together produce 457 TWh yr^{-1} with a maximum GHG footprint of 138 g CO$_2$-eq kWh^{-1}. The majority of power, 455 TWh yr^{-1} (99.6%), is produced with a footprint below 100 g CO$_2$-eq kWh^{-1}, in 9810 facilities. 262 TWh yr^{-1} is produced by current facilities (see figure 4(a)), and 194 TWh yr^{-1} by planned facilities (see figure 4(b)). For current facilities, 7818 out of 7934 facilities (97.9%) have a footprint below 100 g CO$_2$-eq kWh^{-1}. For planned facilities, 1992 out of 2010 (99.1%) have a footprint below 100 g CO$_2$-eq kWh^{-1}.

Furthermore, by applying a bootstrapping technique we find that for current facilities, uncertainty in panel type does not have a strong effect on the GHG emission—supply curve (see figure 4(a)). The spread induced by unknown panel types (difference between the 2.5th and 97.5th percentiles) is less than 5 g CO$_2$-eq kWh^{-1}, and is highest at low footprints (∼10%). Near total cumulative production the spread reduces to ∼1%. For planned facilities, the spread is larger (see figure 4(b)), because a large part of these facilities (94.0%) has an unknown panel type. At low footprints the spread reaches 50%, or 11 g CO$_2$-eq kWh^{-1}. The spread reduces to ∼5% in the upper regions of the emission—supply curve, and reduces further towards the total cumulative production.

3.3. Regression analyses

The best linear regression model to fit the EF$_{GHG}$, based on the facility-specific predictors we take into account, is:

$$\log(\text{EF}_{GHG}) = 65.1 - 0.031 \cdot \text{Year}$$
$$+ \beta_{type} - 0.00025 \cdot I_{mean}$$
$$+ 0.0007 \cdot T_{mean} - 0.0039 \cdot u_{mean}$$
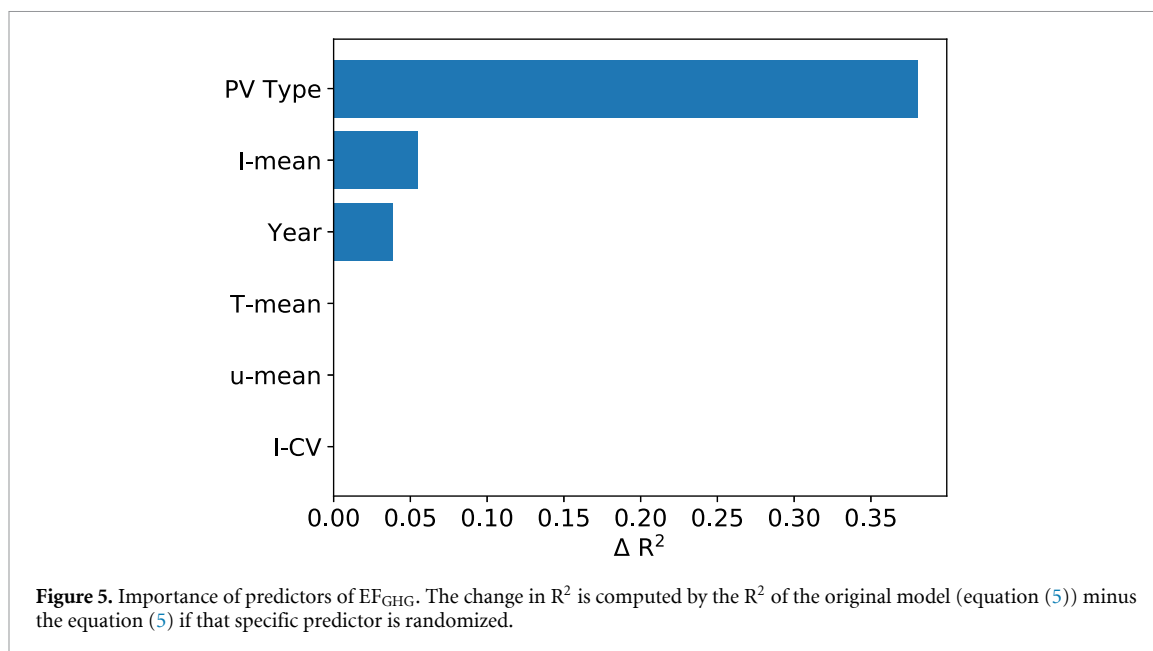$$- 0.17 \cdot I_{CV} + \beta_{Y-type} \cdot \text{Year} \qquad (5)$$

where β_{type} and β_{Y-type} have a type-specific value, because PV panel type is a categorical variable. β_{type} is -48.9 for mono-Si, -48.6 for poly-Si, -13.1 for CdTe, -51.3 for CI(G)S and 0 for a-Si. β_{Y-type} is 0.024 for mono-Si, 0.024 for poly-Si, 0.0064 for CdTe, 0.025 for CI(G)S and 0 for a-Si. The model's R^2 is 0.9868, see SI figure E2. Year should be given in absolute value (i.e. 2009, 2017), irradiation I_{mean} in kWh m^{-2} yr^{-1}, daytime temperature T_{mean} in degrees C, and daytime wind speed u_{mean} in m s^{-1}, I_{CV} as a fraction (see SI section E).

The fact that equation (5) does not include capacity and variation in temperature and wind indicates that these are not important predictors of EF$_{GHG}$ (see SI section E). Randomizing each predictor in equation (5) in turn indicates that PV type is the most important predictor, as the change in R^2 is largest, followed by mean irradiation (see figure 5). Year, or age of facility (used together with panel type to determine panel efficiency) is the third most important predictor of EF$_{GHG}$.

This regression model and importance analyses thus indicates that with only panel type, yearly irradiation and age of a facility, data which should easily be available to a user interested in a specific PV facility, one can quickly make an estimate of the GHG footprint, representing a globally weighted average for PV-producing countries across the world. Reducing the regression model to these three predictors results in the following meta-model:

$$\log(\text{EF}_{GHG}) = 64.3 - 0.031 \cdot \text{Year}$$
$$+ \beta_{type} - 0.00023 \cdot I_{mean}$$
$$+ \beta_{Y-type} \cdot \text{Year} \qquad (6)$$

where β_{type} is -12.7 for CdTe, -49.4 for CI(G)S, 48.9 for mono-Si, 47.6 for poly-Si and 0 for a-Si. β_{Y-type} is 0.0062 for CdTe, 0.025 for CI(G)S, 0.024 for mono-Si, 0.024 for poly-Si and 0 for a-Si. Year should be given

Figure 5. Importance of predictors of EF_{GHG}. The change in R^2 is computed by the R^2 of the original model (equation (5)) minus the equation (5) if that specific predictor is randomized.

in absolute value (i.e. 2009, 2017), irradiation I_{mean} in kWh m^{-2} yr^{-1}. This model has an R^2 of 0.9862, very close to the best model with $R^2 = 0.9868$.

4. Discussion

4.1 Interpretation
Our study confirms that photovoltaic solar power can produce electricity at much lower GHG footprints than fossil fuel, which has footprints in the range of 710–950 g CO_2-eq kWh^{-1} for coal or 410–650 g CO_2-eq kWh^{-1} for gas. When carbon capture and storage (CCS) is considered, the majority of the fossil-based electricity still has a higher footprint than PV (70–290 g CO_2-eq kWh^{-1}) [1, 9].

Compared to published studies or meta-analyses, our footprints are on the same order of magnitude but are generally higher (figure 6). Our range is often larger than that reported in other studies, because we consider a large range of system boundaries such as irradiation and age (efficiency). Some studies also consider a range of system boundaries; see SI tables F1–F4 for parameters used in the literature discussed here and shown in figure 6. Similar ranges of EF_{GHG} are reported by Ludin *et al* [20]. For poly-Si and CdTe they even extend slightly above our values, which could be related to including lower panel efficiencies and shorter lifetimes. Leccisi *et al* [10] also report a range of footprints, representing a range of irradiation similar to ours, as well as production countries. Their lower GHG footprints could be related to higher panel efficiencies (compared to our median values) as well as relatively low impacts I. However, other studies with lower panel efficiencies (such as Hertwich *et al* [15], Bergesen *et al* [9] for CdTe and CI(G)S) also report lower GHG footprints, with similar life times and irradiation, likely related

to different boundary conditions, inventory data or assessment methods. Nian [11] report a similar range, across a similar range of irradiation. High efficiencies may explain why their footprints are overall lower. See SI section F for more details on comparing our footprints to those in literature.

4.2 Production location
One important source of variability in PV environmental footprints, and in different footprints reported in literature, is the location where the panels are produced. Several studies compare footprints of PV produced in different locations, mostly due to different background electricity mixes [10, 11, 13, 19, 24, 38–41]. Furthermore, changes in manufacturing efficiencies and/or import of materials can affect the impacts and footprints for a single production location [12–14, 42, 43]. Of all studies providing footprints (shown in figure 6) and/or impact I we summarized the system boundaries, including production location if provided, in SI tables F1–F4 (see also SI section F). A large range of impact I is shown, often related to production location. Locations (countries) with a low-GHG background electricity mix such as France or Germany are typically associated with low GHG emissions during production (impact I), while countries with electricity mixes strongly based on e.g. coal, such as China, typically have the highest GHG life-cycle emissions. Even for one production country a large range of emissions is reported; for instance for poly-Si from China Leccisi *et al* [10] report 165 kg CO_2-eq m^{-2} while Grant *et al* [41] report 519 kg CO_2-eq m^{-2}.

The exact impact I, and subsequently the GHG footprint, thus strongly depends on the production location as well as the chosen system boundaries, life cycle inventories, impact assessment methods
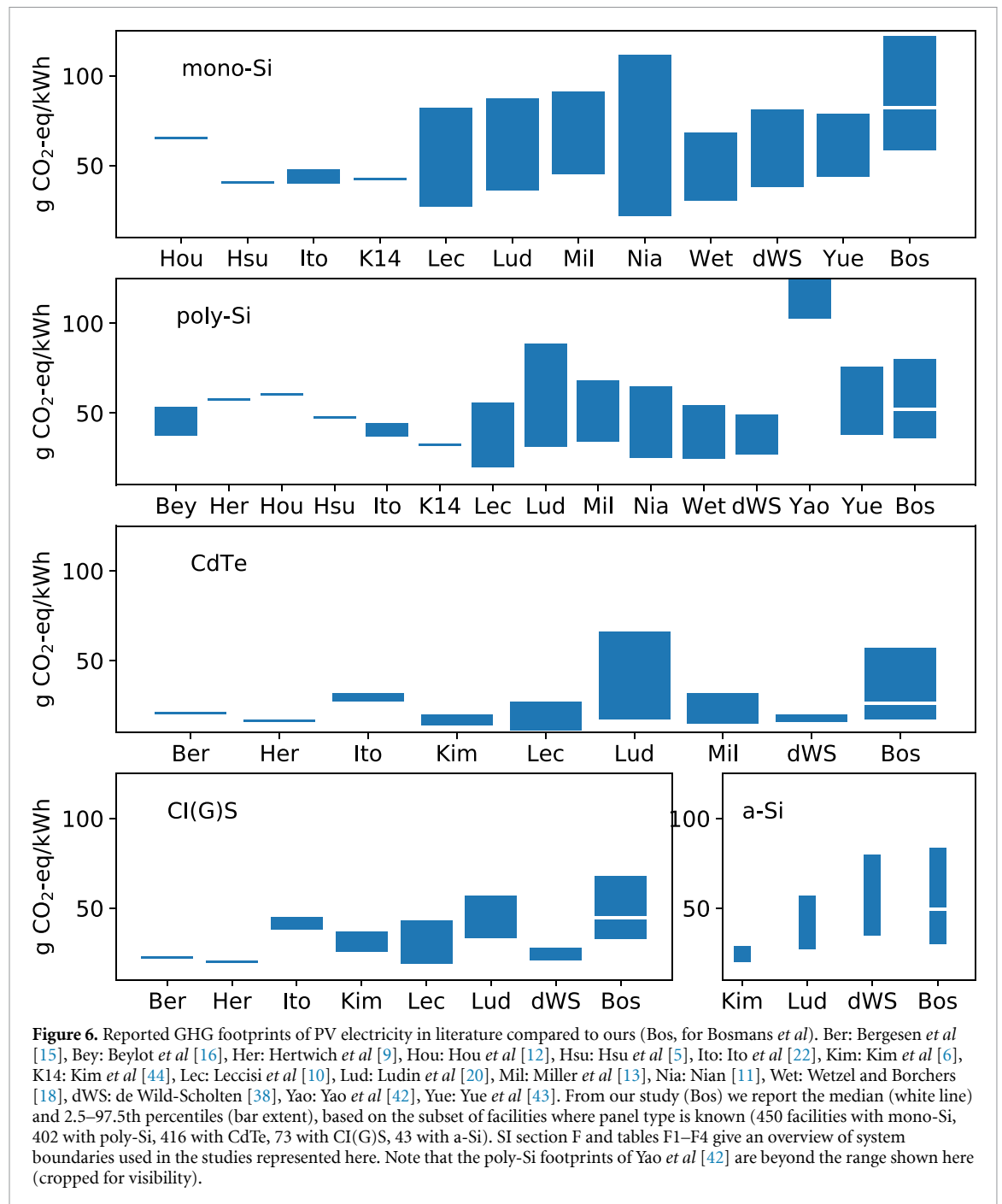
Figure 6. Reported GHG footprints of PV electricity in literature compared to ours (Bos, for Bosmans *et al*). Ber: Bergesen *et al* [15], Bey: Beylot *et al* [16], Her: Hertwich *et al* [9], Hou: Hou *et al* [12], Hsu: Hsu *et al* [5], Ito: Ito *et al* [22], Kim: Kim *et al* [6], K14: Kim *et al* [44], Lec: Leccisi *et al* [10], Lud: Ludin *et al* [20], Mil: Miller *et al* [13], Nia: Nian [11], Wet: Wetzel and Borchers [18], dWS: de Wild-Scholten [38], Yao: Yao *et al* [42], Yue: Yue *et al* [43]. From our study (Bos) we report the median (white line) and 2.5–97.5th percentiles (bar extent), based on the subset of facilities where panel type is known (450 facilities with mono-Si, 402 with poly-Si, 416 with CdTe, 73 with CI(G)S, 43 with a-Si). SI section F and tables F1–F4 give an overview of system boundaries used in the studies represented here. Note that the poly-Si footprints of Yao *et al* [42] are beyond the range shown here (cropped for visibility).

etc [14]. We included variation in production location by using continent-specific weighted averages of the most important production countries based on market shares, but acknowledge that in order to derive facility-specific footprints, more information on facility-specific supply chains is necessary.

Note that we did not include variation in BOS production location. Nian [11] report variation in impacts *I* and footprints for both panels and BOS, showing that changing production location for BOS has an effect, but the effect of changing panel production location is larger. Overall the impacts associated with panels are larger than the impacts associated with BOS, particularly for crystalline panels [14, 44].

4.3 Limitations

A number of assumptions and uncertains may influence our results.

Some of the input (figure 1) was unknown, particularly for panel type. Our results as well as those of others [10, 23] indicate that panel type is an important predictor of EF_{GHG}. We used an average footprint if type is unknown, weighted by production values of the five most common types considered, which we believe results in a representative variation of EF_{GHG} of global PV electricity production. Also, the global emission-supply curve is not strongly affected by uncertainty in panel type. Having more data on panel type will however reduce the uncertainty in facility-specific EF_{GHG}.

When computing life-cycle GHG emissions (I in equation (1)), we did not include facility-specific supply chains, but continent-specific weighted averages of production countries based on market shares. Variation in production location can be an important source of variation in GHG footprints, as described in the previous section. If facility-specific supply chains are known, production country can be added to the regression analysis, improving the prediction of facility-specific GHG footprints.

Another important predictor of EF_{GHG} is panel efficiency. In this study, efficiency varies based on construction year and panel type, but further variation in efficiency can be introduced among different manufacturers or models of the same type. Besides improved panel efficiencies, EF_{GHG} also decreases over time due to improved material and energy utilization in the production process, [e.g. 42, 45]. The latter is not considered in our study.

Furthermore, 'balance of system' components (BOS) were assumed to be the same for all facilities, but we acknowledge that different mounting structures can affect the GHG emissions of a PV facility [7, 16]. We also ignored differences in BOS due to tilt angles or tracking systems. Of all facilities from the Wiki-Solar database, ∼10% uses 1- or 2-way tracking. Although this increases the power output of a facility [46, 47], it also increases environmental impacts due to increased electricity and material needs. Sinha *et al* [47] report that therefore the EF_{GHG} of fixed and tracking systems are comparable, while Leccisi *et al* [10] find that EF_{GHG} is reduced for an East-West-tracking system, particularly for crystalline panels. Miller *et al* [13] find that whether the PV GHG footprint is in- or decreased when a tracking system is included strongly depends on the panel type as well as irradiation and cloud cover.

When computing the life-time electricity output (P in equation (1)), we included location-specific high-resolution climate variables, as well as a loss factor to take panel degradation into account. Using a IEA-recommended fixed loss factor of 0.7% [31] we ignore that panel degradation can vary between locations and panel types [13, 21, 48–50]. We also ignore that power production can be reduced by shading or soiling through e.g. dust or snow as well as faulty installation or lack of maintenance [21, 49, 51, 52]. Third, we assume a fixed lifetime of 30 years for all facilities. A shorter or longer lifetime will directly affect the footprint, as shown by [5, 6, 18]. We use the ERA5 reanalysis data from 1988 to 2017 to obtain a representative power output under current climate. We tested that power output is not sensitive to the exact years chosen; for 1460 locations we compared average power output for 2008–2017 to that of 1988–2017 and found that the difference is less than 1% for 88% of the locations, and all differences are less than 3%. We did not account for the panel type-specific effects of low irradiance, variation in spectral

irradiance or angle of incidence on PV electricity production [37]. Furthermore, our footprint is expressed per kWh produced, while the amount of power ultimately consumed will be lower due to losses in the power grid as well as potential mismatches between PV production and power demand. Adding battery storage would allow for less power losses, but will likely increase environmental footprints, depending on the battery type [53]. The inclusion of batteries may increase payback times and global warming potential by up to 30% [54].

Lastly, we computed electric power output for all facilities assuming flat panels. Louwen *et al* [21], Chen *et al* [55] show that the tilt of a facility can have a large range within which electricity production remains very similar, but we acknowledge that especially at higher latitudes we may underestimate electricity output.

4.4 Outlook

Our conclusions hold for GHG footprints, but this type of analysis could be expanded to other impact categories, such as material scarcity or eco-toxicity. Furthermore, the regression model we built can be used to estimate GHG footprints for individual facilities even with limited input. Computational efforts can be reduced by not using temporarily detailed climate data, as the regression model indicated that climate variables other than mean irradiation do not strongly affect a PV facility's life-cycle GHG footprint. It is however important to fill data gaps concerning the panel type used and production location.

Our GHG emission—supply curves of cumulative PV production can also be used in integrated assessment models (IAMs), in addition to cost-supply curves [56], to include both financial and environmental constraints in renewable energy scenarios. For future scenarios, one should take into account reduced impacts I during manufacturing due to technological advances as well as the decarbonization of energy supply [e.g. 45, 57].

5. Conclusion

In this study we computed the GHG footprint for 9992 utility-scale PV facilities across the globe, based on facility-specific construction year, capacity, panel type and high-resolution climate data, as well as variation in production location. We find utility-scale PV GHG footprints of 58.7 (28.2–94.6) g CO_2-eq kWh^{-1} (median, 2.5–97.5th quantiles). Spatially, locations with higher irradiation logically have lower footprints, but panel type is the most important predictor of EF_{GHG}. Placing a cadmium telluride panel, with low life-cycle GHG emissions, in Europe can result in a lower GHG footprint than placing a monocrystalline silicon panel, with high life-cycle GHG emissions, in South America, despite the much larger

irradiation at facilities in the latter continent [21, 23]. Panel efficiency (here determined through a facilities age) is the third most important predictor of GHG footprints.

We acknowledge that with more data, more accurate facility-specific footprints can be computed. Efforts should mainly focus on adding panel type and production country. We do find that the uncertainty in panel type does not strongly affect the global PV GHG emission—electricity supply curves.

Data availability statement

The data generated and/or analysed during the current study are not publicly available for legal/ethical reasons but are available from the corresponding author on reasonable request.

The facility-specific technological characteristics and locations from Wiki-Solar are proprietory, and can be obtained from https://wiki-solar.org. The continent-specific market shares by origin countries are also proprietory, and can be obtained through https://www.marketreportsworld.com/TOC/12344406#TOC. We used Chapter 8 (Global Solar Photovoltaic (PV) Market Analysis, by Geography)[26]. The climate data used in this study [25] can be obtained from the Copernicus Climate Change Service [35] for free. We used ERA5's hourly single level data.

Acknowledgments

Conflict of interest

We declare that none of the authors have a financial conflict of interest.

This paper is accompanied by Supplementary Information (PaperPV_ERL_final_SI.pdf).

References

[1] Bruckner T, Bashmakov I A, Mulugetta Y and Chum H *et al* 2014 Energy systems, IPCC Working Group 3 Assessment Report 5

[2] IRENA: Renewable capacity statistics 2020 Int. Renewable Energy Agency (IRENA) Abu Dhabi

[3] Int. Energy Agency (I.E.A.): Fuels & Technologies: Solar (available at: www.iea.org/fuels-and-technologies/solar) 2020

[4] Int. Energy Agency (I.E.A.): Solar PV (available at: www.iea.org/reports/solar-pv) 2020

[5] Hsu D D, O'Donoughue P, Fthenakis V, Heath G A, Kim H C, Sawyer P, Choi J-K and Turney D E 2012 Life cycle greenhouse gas emissions of crystalline silicon photovoltaic electricity generation *J. Ind. Ecol.* **16** S1

[6] Kim H C, Fthenakis V, Choi J-K and Turney D E 2012 Life cycle greenhouse gas emissions of thin-film photovoltaic electricity generation *J. Ind. Ecol.* **16** S1

[7] Bhandari K P, Collier J M, Ellingson R J and Apul D S 2015 Energy payback time (EPBT) and energy return on energy invested (EROI) of solar photovoltaic systems: a systematic review and meta-analysis *Renew. Sustain. Energy Rev.* **47** 133–41

[8] Louwen A, Van Sark W G, Faaij A P and Schropp R E 2016 Re-assessment of net energy production and greenhouse gas emissions avoidance after 40 years of photovoltaics development *Nat. Commun.* **7** 13728

[9] Hertwich E G *et al* 2015 Integrated life-cycle assessment of electricity-supply scenarios confirms global environmental benefit of low-carbon technologies *Proc. Natl Acad. Sci.* **112** 6277–82

[10] Leccisi E, Raugei M and Fthenakis V 2016 The energy and environmental performance of ground-mounted photovoltaic systems—a timely update *Energies* **9** 622

[11] Nian V 2016 Impacts of changing design considerations on the life cycle carbon emissions of solar photovoltaic systems *Appl. Energy* **183** 1471–87

[12] Hou G, Sun H, Jian Z, Pan Z, Wang Y, Zhang X, Zhao Y and Yao Q 2016 Life cycle assessment of grid-connected photovoltaic power generation from crystalline silicon solar modules in China *Appl. Energy* **164** 882–90

[13] Miller I, Gençer E, Vogelbaum H S, Brown P R, Torkamani S and OŚullivan F M 2019 Parametric model of life cycle greenhouse gas emissions from photovoltaic power *Appl. Energy* **238** 760–74

[14] Muteri V, Cellura M, Curto D, Franzitta V, Longo S, Mistretta M and Prisi M L 2020 Review on life cycle assessment of solar photovoltaic panels *Energies* **13** 252

[15] Bergesen J D, Heath G A, Gibon T and Suh S 2014 Thin-film photovoltaic power generation offers decreasing greenhouse gas emissions and increasing environmental co-benefits in the long term *Environ. Sci. Technol.* **48** 9834–43

[16] Beylot A, Payet J, Puech C, Adra N, Jacquin P, Blanc I and Beloin-Saint-Pierre D 2014 Environmental impacts of large-scale grid-connected ground-mounted PV installations *Renew. Energy* **61** 2–6

[17] Nugent D and Sovacool B K 2014 Assessing the lifecycle greenhouse gas emissions from solar PV and wind energy: a critical meta-survey *Energy Policy* **65** 229–44

[18] Wetzel T and Borchers S 2015 Update of energy payback time and greenhouse gas emission data for crystalline silicon photovoltaic modules *Prog. Photovolt., Res. Appl.* **23** 1429–35

[19] Gazbour N, Razongles G, Monnier E, Joanny M, Charbuillet C, Burgun F and Schaeffer C 2018 A path to reduce variability of the environmental footprint result of photovoltaic systems *J. Cleaner Prod.* **197** 1607–18

[20] Ludin N A, Mustafa N I, Hanafiah M M, Ibrahim M A, Teridi M A M, Sepeai S, Zaharim A and Sopian K 2018 Prospects of life cycle assessment of renewable energy from solar photovoltaic technologies: a review *Renew. Sustain. Energy Rev.* **96** 11–28

[21] Louwen A, Schropp R E, van Sark W G and Faaij A P 2017 Geospatial analysis of the energy yield and environmental footprint of different photovoltaic module technologies *Sol. Energy* **155** 1339–53

[22] Ito M, Lespinats S, Merten J, Malbranche P and Kurokawa K 2016 Life cycle assessment and cost analysis of very large-scale PV systems and suitable locations in the world *Prog. Photovolt., Res. Appl.* **24** 159–74

[23] Pérez-López P, Gschwind B, Blanc P, Frischknecht R, Stolz P, Durand Y, Heath G, Ménard L and Blanc I 2017 ENVI-PV: an interactive web client for multi-criteria life cycle assessment of photovoltaic systems worldwide *Prog. Photovolt., Res. Appl.* **25** 484–98

[24] Perez-Lopez P, Gschwind B, Frischknecht R, Stolz P, Mehl C, Payeur M, Heath G and Blanc I 2019 Combining region-specific supply chains with geo-located PV electricity production for life cycle assessment of worldwide crystalline silicon photovoltaic systems in ENVI-PV 2.0 *36th European Photovoltaic Solar Conf. and Exhibition Sep 2019 Marseille*

[25] European Centre for Medium-range Weather Forecasts (ECMWF): ERA5 Climate reanalysis (available at: https://climate.copernicus.eu/climate-reanalysis) (accessed 8 October 2019)

[26] Absolute Reports: Global Solar Photovoltaic (PV) Market-Growth, Trends and Forecasts (2018–2023) Chapter 8: Global Solar Photovoltaic (PV) Market Analysis, by Geography (available at: www.marketreportsworld.com/TOC/12344406#TOC) obtained 15 April 2021

[27] Chen Y *et al* 2018 From laboratory to production: learning models of efficiency and manufacturing cost of industrial crystalline silicon and thin-film photovoltaic technologies *IEEE J. Photovol.* **8** 1531–8

[28] Jerez S *et al* 2015 The impact of climate change on photovoltaic power generation in Europe *Nat. Commun.* **6** 10014

[29] Mavromatakis F, Makrides G, Georghiou G, Pothrakis A, Franghiadakis Y, Drakakis E and Koudoumas E 2010 Modeling the photovoltaic potential of a site *Renew. Energy* **35** 1387–90

[30] Stoop L 2018 Blackouts are not an option Master's Thesis Utrecht University, the Netherlands (available at: https://laurensstoop.nl/publication/msc_thesis/)

[31] Frischknecht R, Stolz P, Heath G, Raugei M, Sinha P and de Wild-Scholten M Methodology guidelines on life cycle assessment of photovoltaic electricity, 4th edn, IEA PVPS task 12, *Int. Energy Agency Photovoltaic Power Systems Programme* Report IEA-PVPS T12-18:2020

[32] Fraunhofer Institute for Solar Energy Systems (ISE): Photovoltaics report, Tech. rep, ISE 2019

[33] U.S. Energy Information Administration (E.I.A.): EIA-860 2018 data (available at: www.eia.gov/electricity/data/eia860/) (accessed 30 September 2019)

[34] Gupta R and Shankar H Global energy observatory (GEO) (available at: http://globalenergyobservatory.org/) (accessed 12 November 2019)

[35] Copernicus Climate Change Service: ERA5: Fifth generation of ECMWF atmospheric reanalyses of the global climate (available at: https://cds.climate.copernicus.eu/cdsapp#!/home) Copernicus Climate Change Service (C3S) Climate Data Store (CDS)

[36] Kawajiri K, Oozeki T and Genchi Y 2011 Effect of temperature on PV potential in the world *Environ. Sci. Technol.* **45** 9030–5

[37] Huld T, Gottschalg R, Beyer H G and Topič M 2010 Mapping the performance of PV modules, effects of module type and data averaging *Sol. Energy* **84** 324–38

[38] de Wild-Scholten M M 2013 Energy payback time and carbon footprint of commercial photovoltaic systems *Sol. Energy Mater. Sol. Cells* **119** 296–305

[39] Kawajiri K and Genchi Y 2012 The right place for the right job in the photovoltaic life cycle *Environ. sci. Technol.* **46** 7415–21

[40] Serrano-Luján L, Espinosa N, Abad J and Urbina A 2017 The greenest decision on photovoltaic system allocation *Renew. Energy* **101** 1348–56

[41] Grant C A and Hicks A L 2020 Effect of manufacturing and installation location on environmental impact payback time of solar power *Clean Technol. Environ. Policy* **22** 187–96

[42] Yao Y, Chang Y and Masanet E 2014 A hybrid life-cycle inventory for multi-crystalline silicon PV module manufacturing in China *Environ. Res. Lett.* **9** 114001

[43] Yue D, You F and Darling S B 2014 Domestic and overseas manufacturing scenarios of silicon-based photovoltaics: life cycle energy and environmental comparative analysis *Sol. Energy* **105** 669–78

[44] Kim B, Lee J, Kim K and Hur T 2014 Evaluation of the environmental performance of sc-Si and mc-Si PV systems in Korea *Sol. Energy* **99** 100–14

[45] Fthenakis V and Leccisi E 2021 Updated sustainability status of crystalline silicon-based photovoltaic systems: life-cycle energy and environmental impact reduction trends *Progress Photovol.* **29** 1068–77

[46] Perpiñan O, Lorenzo E, Castro M and Eyras R 2009 Energy payback time of grid connected PV systems: comparison between tracking and fixed systems *Prog. Photovolt., Res. Appl.* **17** 137–47

[47] Sinha P, Schneider M, Dailey S, Jepson C and de Wild-Scholten M 2013 Eco-efficiency of CdTe photovoltaics with tracking systems *2013 IEEE 39th Photovoltaic Conf. (PVSC)* (IEEE) pp 3374–8

[48] Jordan D C and Kurtz S R 2013 Photovoltaic degradation rates—an analytical review *Prog. Photovolt., Res. Appl.* **21** 12–29

[49] Santhakumari M and Sagar N 2020 A review of the environmental factors degrading the performance of silicon wafer-based photovoltaic modules: failure detection methods and essential mitigation techniques *Renew. Sustain. Energy Rev.* **110** 83–100

[50] Kaaya I, Koehl M, Mehilli A P, de Cardona Mariano S and Weiss K A 2019 Modeling outdoor service lifetime prediction of PV modules: effects of combined climatic stressors on PV module power degradation *J. Photovol.* **9** 1105–12

[51] Kim B and Kim C 2018 Estimating the effect of module failures on the gross generation of a photovoltaic system using agent-based modeling *Renew. Sustain. Energy Rev.* **91** 1019–24

[52] Dida M, Slimane B, Bechki D and Bouguettaia H 2020 Output power loss of crystalline silicon photovoltaic modules due to dust accumulation in Saharan environment *Renew. Sustain. Energy Rev.* **124** 109787

[53] Das J, Abraham A P, Ghosh P C and Banerjee R 2018 Life cycle energy and carbon footprint analysis of photovoltaic battery microgrid system in India *Clean Technol. Environ. Policy* **20** 65–80

[54] Raugei M, Leccisi E and Fthenakis V 2020 What are the energy and environmental impacts of adding battery storage to photovoltaics? A generalized life cycle assessment *Energy Technol.* **8** 11

[55] Chen X M, Li Y, Zhao B Y and Wang R Z 2020 Are the optimum angles of photovoltaic systems so important? *Renew. Sustain. Energy Rev.* **124** 109791

[56] Gernaat D E H J, 2019 The role of renewable energy in long-term energy and climate scenarios Ph.D. Thesis University Utrecht

[57] Pehl M, Arvesen A, Humpenöder F, Popp A, Hertwich E G and Luderer G 2017 Understanding future emissions from low-carbon power systems by integration of life-cycle assessment and integrated energy modelling *Na. Energy* **2** 939–45

[58] Hunter J D 2007 Matplotlib: a 2D graphics environment *Comput. Sci. Eng.* **9** 90–5